Bacteriorhodopsin optoelectronic synapses

David P. Shelton

Department of Physics, University of Nevada, Las Vegas, Las Vegas, Nevada 89154-4002

Received July 30, 1997

Synapses are critical components of an artificial neural network. Bacteriorhodopsin thin film can be used to construct compact, finely graded synapses for an optoelectronic neural network, based on its photochromic properties. Measurements show that these photochromic changes are blocked at low temperature. Thermal gating will allow synapses to be written on the film optically and then read without erasure by the same light and also will permit local implementation of an associative learning rule for updating synaptic weights.

In recent years there has been a resurgence of interest in artificial neural networks, and several optical implementations have been investigated,[1–3] including optoelectronic implementations that use bacteriorhodopsin (BR).[4–6] Neural networks are intrinsically parallel computers, and optics can provide the massive parallelism and interconnectivity that they require. The key components of neural networks are the synapses between the neurons. The synapses are the loci of signal processing, learning, and memory. BR has photochromic properties that enable one to construct functionally complete synapses in the form of a thin-film optically addressed spatial light modulator[7,8] as part of an optoelectronic neural network. Here I present measurements of some properties of BR relevant to synaptic functions and describe the BR artificial synapses that can be constructed.

The BR photocycle is shown in Fig. 1.[9–11] Absorption of a photon at $\lambda = 570$ nm converts a BR molecule from the yellow-absorbing ground state (B) to the relatively long-lived blue-absorbing state (M). The absorption spectra of the B and M states are shown in Fig. 2. Either thermally activated relaxation processes or the absorption of a blue photon will return the molecule from the M state to the B state, completing the photocycle. The protein part of BR ensures stereoselective and reversible photoisomerization of the retinal chromophore with high quantum yield and without side reactions. A key feature, in the present context, is that one can switch off the forward (B → M) and the reverse (M → B) photoreactions by lowering the temperature of the BR film.[9,10,12] This allows one to write a pattern on the film with a light beam and then read out the pattern without erasure, by using the same light beam.

The temperature dependence of the forward and reverse photoreactions was studied by measurement of the changes in the B-state optical absorbance of BR film illuminated by yellow or blue light. The techniques are similar to those previously described[13] but with measurements made over a wider temperature range. The sample film was mounted in a variable-temperature optical cryostat and could be illuminated with several overlapping light beams, as shown in Fig. 3. The sample absorbance was measured *in situ* with a fiber-coupled CCD spectrometer to monitor the spectral transmission of a 5-μW/cm^2 white-light probe beam. In the first experiment the sample was prepared in the B state and cooled to the desired temperature. Then the sample was illuminated for as long as 10 min with a cw dye laser beam at $\lambda = 590$ nm with an intensity of ~100 mW/cm^2, and the absorbance change at 560 nm was measured. At temperatures below 150 K a short exposure to an additional 686-nm 100-mW/cm^2 laser beam was used to drive molecules trapped in the first long-lived intermediate state (K in Fig. 1) back into the B state before the absorbance change was measured. In the second experiment the sample was prepared in the M state by use of the 590-nm pump beam and cooled to the desired temperature. Then the sample was illuminated with a 3-ns 1-mJ/cm^2 flash of blue light at 410 nm from a pulsed dye laser, and the time course and the amplitude of the absorbance change seen by a 543.5-nm 1-mW/cm^2 probe laser beam were measured with 50-ns time resolution with a photomultiplier tube and a digital sampling oscilloscope.

The results of these measurements for a wild-type BR–polymer film 0.4 mm thick are shown in Fig. 4. The film was produced by Bend Research and has peak optical density 2.0 at 570 nm. The film was prepared with high pH to increase the M-state lifetime to 4 s. At temperatures above 200 K both the forward and the reverse photoreactions are fully enabled. The observed absorbance change that was due to the M → B reverse photoreaction following a light flash at 290 K is a simple exponential relaxation with $t_{1/2} = 150$ ns. As the temperature is lowered, the reverse photoreaction becomes slower and the observed transient shows

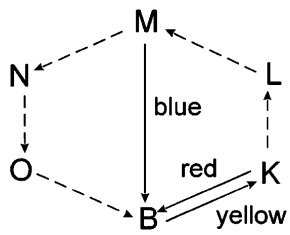

Fig. 1. Photocycle of light-adapted BR with photoreactions shown as solid lines and thermally activated reactions shown as dashed lines. The spectroscopically distinguishable intermediate states K, L, N, and O are short-lived compared with M. The key states in the BR photocycle for this application are B, K, and M.

0146-9592/97/221728-03$10.00/0

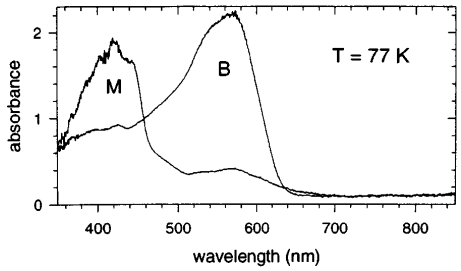

Fig. 2. Absorption spectra of BR film at 77 K in the B and M states.

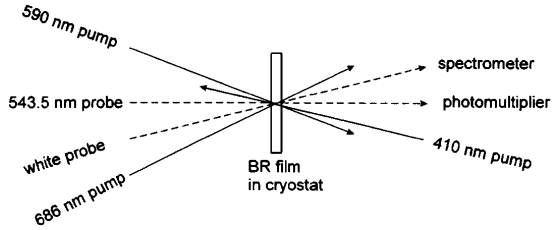

Fig. 3. Schematic of the experimental apparatus. Pump (solid lines) and probe (dashed lines) light beams intersect in the BR sample.

multiexponential relaxation with a wide range of time scales (the relaxation at 170 K is composed of 700-ns and 70-μs components of approximately equal amplitude). Below 100 K the photoreactions are disabled. The forward and the reverse reactions show approximately the same temperature dependence. The first step of the forward photoreaction, the transition between B and K, is not blocked, even at 77 K.

Previous research showed that the quantum efficiencies for the forward and the reverse photoreactions at room temperature are near unity.[9,10] Therefore, the fluence needed to completely write or erase a BR film with peak absorbance $A = 2.0$ is $\sim$10 mJ/cm^2 at room temperature. The stoichiometry of approximately one photon per molecule per photochromic reaction limits the writing speed of a simple BR memory unless high intensities are used. For neural network applications, in which a succession of small incremental changes in the synaptic weights occurs during training, there is a good match to the slow but finely graded writing at low intensity by photobleaching that BR offers. Once they are written, it is also important that the synaptic weights be stabilized against erasure by light during operation of the neural network. The degree to which the forward and the reverse photoreactions are disabled at 77 K was determined from the absorbance changes measured following extended periods of illumination with yellow or blue light (2-kJ/cm^2 or 20-J/cm^2 fluence, respectively). The total observed absorbance changes at 570 nm were -0.1 or $+0.5$, respectively, with the absorbance change per unit fluence decreasing steeply as photobleaching proceeded. Extrapolating the observations, the fluence to produce an absorbance change $\Delta A_{570} = 2.0$ is estimated to be $>$100 kJ/cm^2 for the forward reaction, B $\rightarrow$ M, and $\sim$200 J/cm^2 for the reverse reaction, M $\rightarrow$ B. The corresponding quantum efficiencies are $<10^{-7}$ and $\approx 10^{-4}$, respectively. The B $\rightarrow$ M photoreaction is effectively disabled at 77 K.

BR can be used in construction of the synapses for neurons in an optoelectronic neural network, as shown in Fig. 5. The input light beams pass through the BR film, where the synaptic weights are written as a pattern of optical transmittance, and the transmitted light beams are summed by a photodetector. An electronic circuit processes the detector output and drives a laser output device. The synaptic weights remain fixed while the BR film is maintained at low temperature. Learning in the neural network is enabled when the temperature of the BR film is raised, so the input light beams can change the transmittance of the BR film. The learning-enabling response time is limited by thermal inertia and can be reduced by use of a pure BR film to minimize the thickness of the synaptic layer. The thermal switching time for a 5-μm-thick BR film with a 3-W/cm^2 heater is $\sim$20 ms.

Effective learning rules for modifying the synaptic weights of the network to achieve a desired function are critical to most neural network applications.[14] Signal-processing functions approaching the sophistication of biological synapses[15] can be achieved if the neuron

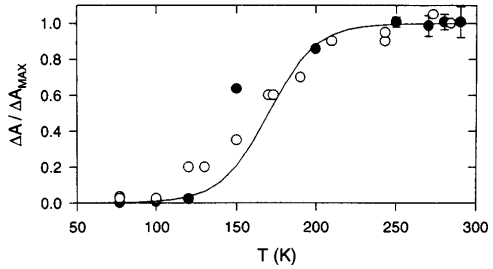

Fig. 4. Normalized B-state absorbance change versus temperature measured for wild-type BR/polymer film. Filled and open circles show measurements of the change in the absorbance peak for the B state owing to forward (B $\rightarrow$ M) and reverse (M $\rightarrow$ B) photoreactions, respectively. The fitted curve is the function $F(T) = \{1 + \exp[(T - 170)/15]\}^{-1}$.

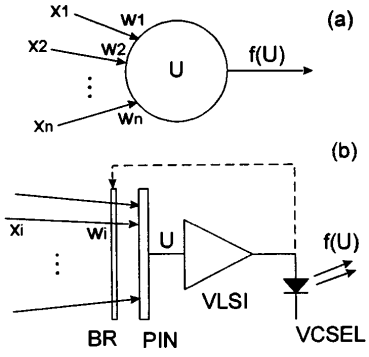

Fig. 5. Schematics of (a) a generic neuron and (b) an optoelectronic neuron, with optical inputs x_i, synaptic weights w_i, neuron electrical activation $U \propto \sum_i w_i x_i$, and neuron optical output $f(U)$. The synapses are implemented with a BR film (BR) and a photodiode (PIN), whose output goes to an integrated circuit (VLSI), which drives a laser (VCSEL). The dashed line indicates a path for control signals from the neuron back to the overlying synaptic layer.

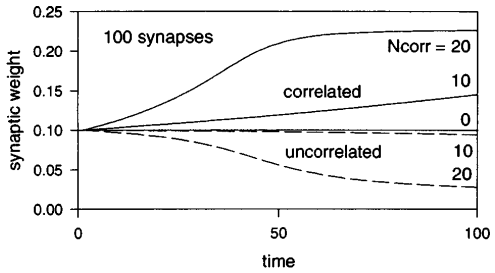

Fig. 6. Synaptic weight evolution calculated for a model neuron when the activation of a subset of the synapses, N_{corr} in number, is correlated. The synaptic input intensity is random and binary, $x_i = 0$ or $x_i = 1$, with average ON time of 10% for all synapses. The synapses in the correlated subset are activated only simultaneously. The time evolution of the weights for synapses with correlated and uncorrelated inputs (solid and dashed curves, respectively), calculated with the mean-field approximation for cases with 0, 10, and 20 synchronously activated synapses, is shown. Only the synapses with correlated activity are reinforced. The model for the ith synapse is $w_i = \exp[(f_i - 1)A_0 \ln 10]$, $\mathrm{d}f_i/\mathrm{d}t = [x_i(1 - f_i) - bf_i]F(T)$, and $F(T) = \{1 + \exp[-(T - 170)/15]\}^{-1}$, where $A_0 = 2.0$, x_i and b are the yellow- and blue-light intensities, respectively, at the synapse, and $f_i = [M]_i/([B]_i + [M]_i)$ is the fraction of photobleached BR molecules. The model for the neuron is $U = g\sum_i w_i x_i$, $T = (200U + 77)$, and $b = U$, where the neuron gain is $g = 0.10$ and there are 100 synapses.

shown in Fig. 5 is modified to send control signals back to the overlying BR synaptic layer. In this example the neuron drives a yellow laser to send information to other neurons and also a blue laser and a heater to control the overlying BR synaptic layer. (Only yellow light is allowed to reach the photodetector, and a red floodlight for the entire BR film may also be needed to prevent the buildup of a population trapped in the K state.) In this model the temperature and the intensity of the blue light falling upon the BR film increase linearly with the neuron activation. As a result, the effect of a yellow input light beam depends on the degree of neuron activation.

Figure 6 shows an example of unsupervised associative learning by this model neuron. With uniform random inputs the synaptic weights remain constant because there is a balance between writing by the yellow input light and erasure by the blue control light at the operating point. This balance is disturbed when some of the synapses have correlated inputs, so synapses with correlated activity are reinforced whereas synapses with uncorrelated activity are weakened. The neuron learns to respond preferentially to inputs with a mutual association. One can freeze the updated pattern of weights at any time by disabling the BR heater. Note that activity-dependent thermal modulation of the BR photoreactions is essential for associative learning. The synapses are independently updated in parallel, saturation of the synaptic weights is avoided because synaptic weights can decrease as well as increase, and the synapses can be as small as the diffraction limit allows.

The BR synapses described here can form a two-dimensional array with a density up to $10^8/\mathrm{cm}^2$. An advantage of these two-dimensional synapses is that each is distinct and proximate to the neuron that it derives, which permits versatile local control of synaptic modification, in contrast to neural networks in which the synaptic weights are stored in distributed form in three dimensions in photorefractive crystals. Simple, compact BR synapses that use thermally gated photochromism are able to store finely graded analog weights and perform complex signal-processing functions. Synapses with these properties will be key components in large-scale artificial neural networks.

References

1. M. Balberg, M. Razvag, S. Vidro, E. Rafaeli, and A. J. Agranat, Opt. Lett. **21,** 1544 (1996).
2. K. Wagner and D. Psaltis, eds., feature on optical implementation of neural networks, Appl. Opt. **32,** 1261–1476 (1993).
3. D. Psaltis, D. Brady, X. G. Gu, and S. Lin, Nature (London) **343,** 325 (1990).
4. D. Haronian and A. Lewis, Appl. Opt. **30,** 97 (1991).
5. H. Takei, A. Lewis, Z. Chen, and I. Nebenzahl, Appl. Opt. **30,** 500 (1991).
6. H. Takei and N. Shimizu, Opt. Lett. **21,** 537 (1996).
7. R. Thoma, N. Hampp, C. Brachle, and D. Oesterhelt, Opt. Lett. **16,** 651 (1991).
8. Q. W. Song, C. Zhang, R. Blumer, R. B. Gross, Z. Chen, and R. R. Birge, Opt. Lett. **18,** 1373 (1993).
9. D. Oesterhelt, C. Brauchle, and N. Hampp, Q. Rev. Biophys. **24,** 425 (1991).
10. R. R. Birge, Annu. Rev. Phys. Chem. **41,** 683 (1990).
11. J. K. Lanyi, in *Molecular and Biomolecular Electronics*, R. R. Birge, ed., Vol. 240 of Advances in Chemistry (American Chemical Society, Washington, D.C., 1994), Chap. 20, p. 491.
12. S. P. Balashov and F. F. Litvin, Biophysics **25,** 566 (1981).
13. M. Bacon, C. H. Wang, A. K. Kar, R. L. Baxter, and B. S. Wherett, Opt. Commun. **124,** 175 (1996).
14. S. Haykin, *Neural Networks* (Macmillan, Englewood Cliffs, N.J., 1994).
15. T. H. Brown and S. Chattrji, in *Models of Neural Networks II*, E. Domany, J. L. van Hemmen, and K. Schulten, eds. (Springer, New York, 1994), Chap. 8, p. 287.